

DNA Polymerase Epsilon Deficiency Causes IMAGe Syndrome with Variable Immunodeficiency

Clare V. Logan,^{1,32} Jennie E. Murray,^{1,2,32,*} David A. Parry,¹ Andrea Robertson,¹ Roberto Bellelli,³ Žygimantė Tarnauskaitė,¹ Rachel Challis,^{1,2} Louise Cleal,^{1,2} Valerie Borel,³ Adeline Fluteau,¹ Javier Santoyo-Lopez,⁴ SGP Consortium, Tim Aitman,⁵ Inês Barroso,⁶ Donald Basel,⁷ Louise S. Bicknell,⁸ Himanshu Goel,^{9,10} Hao Hu,¹¹ Chad Huff,¹¹ Michele Hutchison,¹² Caroline Joyce,¹³ Rachel Knox,¹⁴ Amy E. Lacroix,¹⁵ Sylvie Langlois,¹⁶ Shawn McCandless,¹⁷ Julie McCarrier,⁷ Kay A. Metcalfe,¹⁸ Rose Morrissey,¹⁹ Nuala Murphy,²⁰ Irène Netchine,²¹ Susan M. O'Connell,²⁰ Ann Haskins Olney,¹⁵ Nandina Paria,²² Jill A. Rosenfeld,²³ Mark Sherlock,²⁴ Erin Syverson,⁷ Perrin C. White,²⁵ Carol Wise,^{22,25,26,27} Yao Yu,¹¹ Margaret Zacharin,²⁸ Indraneel Banerjee,²⁹ Martin Reijns,¹ Michael B. Bober,³⁰ Robert K. Semple,^{14,31} Simon J. Boulton,³ Jonathan J. Rios,^{22,25,26,27} and Andrew P. Jackson^{1,*}

During genome replication, polymerase epsilon (Pol ϵ) acts as the major leading-strand DNA polymerase. Here we report the identification of biallelic mutations in *POLE*, encoding the Pol ϵ catalytic subunit POLE1, in 15 individuals from 12 families. Phenotypically, these individuals had clinical features closely resembling IMAGe syndrome (intrauterine growth restriction [IUGR], metaphyseal dysplasia, adrenal hypoplasia congenita, and genitourinary anomalies in males), a disorder previously associated with gain-of-function mutations in *CDKN1C*. POLE1-deficient individuals also exhibited distinctive facial features and variable immune dysfunction with evidence of lymphocyte deficiency. All subjects shared the same intronic variant (c.1686+32C>G) as part of a common haplotype, in combination with different loss-of-function variants in *trans*. The intronic variant alters splicing, and together the biallelic mutations lead to cellular deficiency of Pol ϵ and delayed S-phase progression. In summary, we establish *POLE* as a second gene in which mutations cause IMAGe syndrome. These findings add to a growing list of disorders due to mutations in DNA replication genes that manifest growth restriction alongside adrenal dysfunction and/or immunodeficiency, consolidating these as replisome phenotypes and highlighting a need for future studies to understand the tissue-specific developmental roles of the encoded proteins.

DNA replication is a fundamental cellular process necessary to ensure the faithful transmission of genetic information. In eukaryotes, three highly conserved DNA polymerases, polymerase epsilon, delta, and alpha, act in concert at the replication fork. Polymerase epsilon (Pol ϵ) is the major enzyme responsible for the synthesis of the leading strand¹ and is consequently an essential gene.² *POLE* encodes the catalytic subunit of Pol ϵ (POLE1), and somatic and germline missense mutations affecting the proofreading domain of POLE1 have been associated with colon and endometrial cancer.^{3–6}

Microcephalic primordial dwarfism comprises a group of prenatal-onset extreme growth disorders characterized by intrauterine growth retardation, short stature, and microcephaly. Genes involved in cell cycle progression, including multiple components of the replication licensing machinery, have been identified as monogenic causes of this disorder.^{7–11} As the molecular basis for many affected individuals remains to be determined, we performed whole-genome sequencing studies to identify further genes and facilitate more comprehensive diagnosis.

¹MRC Human Genetics Unit, MRC Institute of Genetics and Molecular Medicine, University of Edinburgh, Edinburgh EH4 2XU, UK; ²South East Scotland Clinical Genetics Service, Western General Hospital, Edinburgh EH4 2XU, UK; ³The Francis Crick Institute, 1 Midland Road, London NW1 1AT, UK; ⁴Edinburgh Genomics Clinical Division, University of Edinburgh, The Roslin Institute, Edinburgh EH25 9RG, UK; ⁵MRC Centre for Genomic & Experimental Medicine, MRC Institute of Genetics and Molecular Medicine, University of Edinburgh, Edinburgh EH4 2XU, UK; ⁶Wellcome Sanger Institute, Cambridge CB10 1SA, UK; ⁷Medical College of Wisconsin from Children's Hospital of Wisconsin, Milwaukee, WI 53226, USA; ⁸Department of Pathology, Dunedin School of Medicine, University of Otago, Dunedin 9016, New Zealand; ⁹Hunter Genetics, Waratah, NSW 2305, Australia; ¹⁰University of Newcastle, Callaghan, NSW 2308, Australia; ¹¹Department of Epidemiology, MD Anderson Cancer Center, Houston, TX 77030, USA; ¹²Department of Pediatrics, University of Arkansas, Little Rock, AR 72205, USA; ¹³Department of Clinical Biochemistry, Cork University Hospital, Cork, Ireland; ¹⁴MRC Metabolic Diseases Unit, University of Cambridge, Cambridge CB2 0QQ, UK; ¹⁵University of Nebraska Medical Centre, Omaha, NE 68918, USA; ¹⁶Department of Medical Genetics, The University of British Columbia, Vancouver, BC V6H 3N1, Canada; ¹⁷Pediatric Genetics, UH Cleveland Medical Center, Cleveland, OH 44106, USA; ¹⁸Manchester Centre for Genomic Medicine, Manchester University NHS Foundation Trust and Institute of Human Development, University of Manchester, Manchester M13 9WL, UK; ¹⁹Department of Paediatrics and Child Health, Cork University Hospital, Cork, Ireland; ²⁰UCD School of Medicine, Children's University Hospital, Temple St, Dublin, Ireland; ²¹Sorbonne Université, INSERM, UMR_S 938, APHP, Hôpital Trousseau, 75012 Paris, France; ²²Sarah M. and Charles E. Seay Center for Musculoskeletal Research, Texas Scottish Rite Hospital for Children, Dallas, TX 75219, USA; ²³Department of Molecular and Human Genetics, Baylor College of Medicine, Houston, TX 77030, USA; ²⁴Department of Endocrinology, Beaumont Hospital, Dublin, Ireland; ²⁵Department of Pediatrics, University of Texas Southwestern Medical Center, Dallas, TX 75390, USA; ²⁶Department of Orthopaedic Surgery, University of Texas Southwestern Medical Center, Dallas, TX 75390, USA; ²⁷McDermott Center for Human Growth and Development, University of Texas Southwestern Medical Center, Dallas, TX 75390, USA; ²⁸Division of Medicine, Royal Children's Hospital, Melbourne, VIC 3052, Australia; ²⁹Department of Paediatric Endocrinology, Royal Manchester Children's Hospital, Manchester Academic Health Science Centre, Manchester M13 9WU, UK; ³⁰Nemours-Alfred I. duPont Hospital for Children, Wilmington, DE 19803, USA; ³¹Centre for Cardiovascular Science, University of Edinburgh, Edinburgh EH16 4JT, UK

³²These authors contributed equally to this work

*Correspondence: jennie.murray@igmm.ed.ac.uk (J.E.M.), andrew.jackson@igmm.ed.ac.uk (A.P.J.)

<https://doi.org/10.1016/j.ajhg.2018.10.024>

© 2018 The Authors. This is an open access article under the CC BY-NC-ND license (<http://creativecommons.org/licenses/by-nc-nd/4.0/>).



Table 1. Biallelic *POLE* Mutations (GenBank: NM_006231.3)

| ID | Fam | Sex | Allele 1 | | | Allele 2 | | | Mat Allele | Pat Allele | Country of Origin |
|-----|-----|-----|-------------------|---------------------------------|----------|-------------------|------------------------|----------|------------|------------|-------------------|
| | | | Nucleotide Change | Amino Acid Consequence | MAF | Nucleotide Change | Amino Acid Consequence | MAF | | | |
| P1 | 1 | M | c.2091dupC | p.Phe699Valfs*11 | 0 | c.1686+32C>G | p.Asn563Valfs*16 | 0.000071 | 1 | 2 | UK |
| P2 | 1 | F | c.2091dupC | p.Phe699Valfs*11 | 0 | c.1686+32C>G | p.Asn563Valfs*16 | 0.000071 | 1 | 2 | UK |
| P3 | 2 | M | c.62+1G>A | Essential Splice Site Intron 1 | 0 | c.1686+32C>G | p.Asn563Valfs*16 | 0.000071 | 2 | 1 | Ireland |
| P4 | 3 | F | c.5940G>A | p.Trp1980* | 0.000016 | c.1686+32C>G | p.Asn563Valfs*16 | 0.000071 | 2 | 1 | Australia |
| P5 | 4 | M | c.4728+1G>T | Essential Splice Site Intron 36 | 0 | c.1686+32C>G | p.Asn563Valfs*16 | 0.000071 | 2 | 1 | USA |
| P6 | 5 | F | c.3264_3275+13del | Essential Splice Site Intron 26 | 0.000016 | c.1686+32C>G | p.Asn563Valfs*16 | 0.000071 | 1 | 2 | Canada |
| P7 | 6 | M | c.1A>T | p.? | 0.000081 | c.1686+32C>G | p.Asn563Valfs*16 | 0.000071 | n/a | n/a | USA |
| P8 | 7 | M | c.1A>T | p.? | 0.000081 | c.1686+32C>G | p.Asn563Valfs*16 | 0.000071 | 2 | 1 | Ireland |
| P9 | 7 | F | c.1A>T | p.? | 0.000081 | c.1686+32C>G | p.Asn563Valfs*16 | 0.000071 | 2 | 1 | Ireland |
| P10 | 8 | F | c.3019G>C | p.Ala1007Pro | 0.000009 | c.1686+32C>G | p.Asn563Valfs*16 | 0.000071 | 1 | 2 | Ireland |
| P11 | 9 | F | c.5265delG | Ile1756Serfs*5 | 0 | c.1686+32C>G | p.Asn563Valfs*16 | 0.000071 | 2 | 1 | Australia |
| P12 | 9 | M | c.5265delG | Ile1756Serfs*5 | 0 | c.1686+32C>G | p.Asn563Valfs*16 | 0.000071 | 2 | 1 | Australia |
| P13 | 10 | F | c.2049C>G | p.Tyr683* | 0.000028 | c.1686+32C>G | p.Asn563Valfs*16 | 0.000071 | 1 | 2 | Australia |
| P14 | 11 | M | c.6518_6519delCT | p.Ser2173Phefs*130 | 0.000089 | c.1686+32C>G | p.Asn563Valfs*16 | 0.000071 | 2 | 1 | USA |
| P15 | 12 | M | c.801+2T>C | Essential Splice Site Intron 8 | – | c.1686+32C>G | p.Asn563Valfs*16 | 0.000071 | 1 | 2 | USA |

Abbreviations: ID, individual number; Fam, family number; Mat, maternal; Pat, paternal; n/a, not available. All subjects harbored a loss-of-function mutation in combination with an intronic variant on the alternate allele identified as part of a shared haplotype and found to alter splicing in RNA studies. MAF indicates minor allele frequency in European (non-Finnish) population observed in gnomAD. None of the variants were present in any Non-European population in gnomAD.

Whole-genome sequencing (WGS) of 48 individuals with microcephalic primordial dwarfism identified heterozygous *POLE* (GenBank: NM_006231.3) loss-of-function (LoF) variants in three subjects (P1, P3, P4; Table 1). These LoF variants were significantly enriched in our cohort compared to a control WGS dataset (GnomAD,¹² $p = 5.1 \times 10^{-5}$, Fisher's exact test, Table S1). As these variants were present in the unaffected parents, the WGS data were further evaluated and a second rare intronic variant in *POLE* identified, c.1686+32C>G (dbSNP: rs762985435). This was present in *trans* with the LoF mutation in all three probands (Table 1). Targeted sequencing of *POLE* and interrogation of existing whole-exome sequencing (WES) data in additional cases of primordial dwarfism identified five additional subjects compound heterozygous for LoF alleles and the c.1686+32C>G variant (P5–P9, Table 1). Notably, a clinical diagnosis of IMAGE syndrome (GeneReviews in Web Resources) (MIM: 614732) had been considered in individuals P1 and P3, with adrenal failure also reported in P5, P6, and P7. We therefore investigated cases of IMAGE syndrome drawn from other cohorts without an existing molecular diagnosis (i.e., *CDKN1C* mutation negative). These included three previously published IMAGE-affected case subjects.^{13,14} Analysis of their WGS data identified additional *POLE* LoF variants inherited in *trans* with the in-

tronic variant in individuals P11–P15 (Table 1). The c.1686+32C>G variant was part of a common haplotype in all individuals where WES/WGS performed, extending over 921 kbp (Figure S2, chr12:132341818–133263107, GRCh38). In P10 a missense variant (c.3019G>C) encoding a p.Ala1007Pro substitution was found, at a residue conserved to yeast (Figure S1) within the polymerase domain of the protein (Figure 1). All variants identified were sufficiently rare (MAF < 0.0001¹²) and, where DNA available, segregation in families was consistent with an autosomal recessively inherited disorder (Table 1).

Phenotypically, affected individuals had severe growth failure of prenatal onset (Figure 2, Table S2). IUGR was present in all case subjects (birth weight was -3.0 ± 0.8 SD) with significant short stature evident postnatally (height -8.1 ± 2.4 SD). While head circumference was also significantly reduced (OFC -5.4 ± 1.5 SD), this was less severe, resulting in a relative macrocephaly. Those affected had a common facial appearance with micrognathia, crowded dentition, long thin nose, short wide neck, and small, low-set, posteriorly rotated ears (Figure 2). 12 individuals had adrenal insufficiency and all affected males had genitourinary abnormalities including bilateral cryptorchidism and/or hypospadias, with the majority of case subjects fulfilling clinical criteria for IMAGE syndrome (GeneReviews in Web Resources; Table 2, Table S3, Supplemental Note).

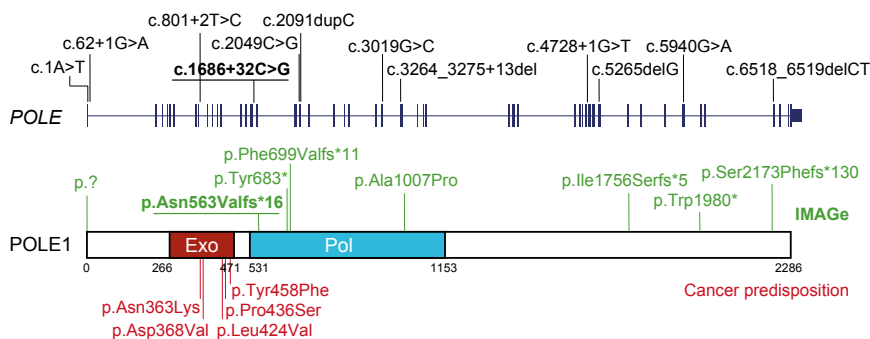


Figure 1. Mutations Causing *POLE*-Associated IMAGe Syndrome Are Distinct from Mutations Conferring a Non-syndromic Susceptibility to Cancer

Schematic of the *POLE* gene, which encodes POLE1, the catalytic subunit of DNA polymerase epsilon. Domains: Pol, polymerase; Exo, exonuclease. Mutations identified in *POLE* subjects indicated above gene and protein (green). Recurrent intronic mutation underlined. For comparison, heterozygous germline missense mutations located in the exonuclease domain predisposing to colorectal cancer and other malignancies highlighted below (red).

Osteopenia and developmental dysplasia of the hip (DDH) were frequently observed and café-au-lait patches were notably present in a third of individuals.

A single homozygous intronic variant (c.4444+3A>G) in *POLE* has previously been reported to be associated with immunodeficiency, lymphopenia, and short stature (facial dysmorphism, immunodeficiency, livedo, and short stature, aka FILS syndrome [MIM: 615139]).^{15,16} Five affected individuals identified in this study also had increased susceptibility to respiratory tract infections, with lymphocyte subset deficiencies and/or IgM hypogammaglobulinemia identified in P1, P3, P4, P8, P9, P14, and P15 (Table 2, Table S4). Deficiency of natural killer cells was present in P1, P3, and P8. P1 had the most profound immunodeficiency, developing CMV pneumonitis and then subsequently developed EBV haemophagocytic lymphohistiocytosis, requiring an allogeneic bone marrow transplant. Notably, this subject's sister (P2), who had the same compound heterozygous *POLE* mutations, died at 22 months from HSV infection. Therefore, our findings

establish that the phenotype spectrum of biallelic *POLE* mutations extends from IMAGe syndrome to include immunodeficiency, in line with the phenotype and pathogenicity of the previously reported c.4444+3A>G mutation.^{15,16}

To establish whether the c.1686+32C>T variant affected the *POLE* transcript, RNA studies were performed on primary fibroblast lines derived from two subjects (P1, P3). RT-PCR using primers spanning *POLE* intron 15 demonstrated the presence of a larger PCR product (Figure 3), which capillary sequencing established to be due to retention of part of intron 15 within *POLE* transcripts (Figure S3). A minigene assay was then performed to assess splicing of this genomic segment and to directly confirm the contribution of the c.1686+32C>G variant. This demonstrated that the c.1686+32C>G variant markedly impaired splicing of the usual exon 15 splice donor site, leading to preferential use of a downstream alternate splice donor site in intron 15, although some canonical splicing also occurred (Figure 3). The inclusion of 47 bp of intronic

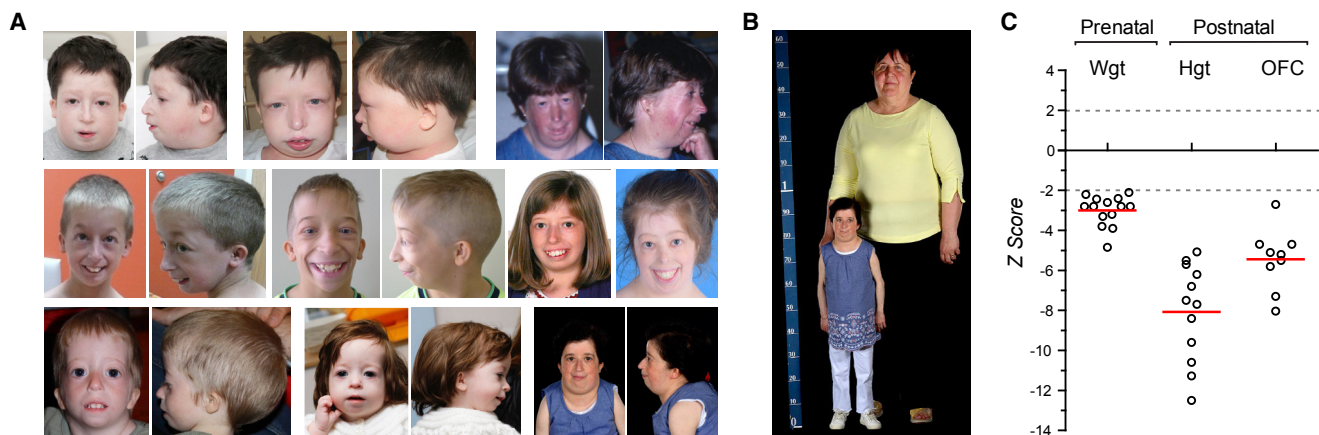


Figure 2. Individuals with Biallelic *POLE* Mutations Have Severely Impaired Pre- and Post-natal Growth and a Recognizable Facial Gestalt

(A) Photographs of *POLE*-deficient subjects demonstrating facial similarities. Written consent obtained from all families for photography.

(B and C) Severe pre-natal onset growth restriction occurs in *POLE*-deficient individuals.

(B) Adult *POLE*-deficient subject next to a control individual of average stature.

(C) Growth is severely impaired pre- and postnatally. Z-scores (standard deviations from population mean for age and sex) for birth weight and postnatal height and head circumference (OFC). Dashed lines 95% confidence interval for general population. Circles, individual subject data points; red bars, mean values.

Table 2. Individuals with Biallelic Mutations in *POLE* Were Clinically Diagnosed with Primordial Dwarfism and Features of IMAGE Syndrome

| ID | Fam | Sex | Age | I | M _{+SI} | A | Ge | -I | Other Features |
|-----|-----|-----|-----|---|------------------|---|----|----|---|
| P1 | 1 | M | 18 | Y | Y | Y | Y | Y | scoliosis, osteopenia, small patella, seizures, gastrostomy, eczema |
| P2 | 1 | F | 1 | Y | Y | Y | - | Y | - |
| P3 | 2 | M | 7 | Y | Y | Y | Y | Y | midline accessory incisor, osteopenia, infant eczema |
| P4 | 3 | F | 50 | Y | Y | N | - | Y | IgM paraproteinaemia |
| P5 | 4 | M | 12 | Y | NA | Y | Y | Y | hypopituitarism, T cell lymphoma, gastrostomy, absent patella |
| P6 | 5 | F | 10 | Y | Y | Y | - | Y | bilat coxa valga, 11 ribs, 6 lumbar vertebrae, scoliosis, gastrostomy, infant eczema |
| P7 | 6 | M | 13 | Y | Y | Y | Y | N | hypopituitarism, atrial septal defect, brachydactyly, gastrostomy |
| P8 | 7 | M | 3 | Y | Y | N | Y | Y | DDH, gastrostomy |
| P9 | 7 | F | 2 | Y | Y | N | - | Y | DDH, gastrostomy |
| P10 | 8 | F | 39 | Y | Y | Y | - | N | DDH, 11 ribs, clinodactyly, osteopenia, café au lait patches |
| P11 | 9 | F | 0.2 | Y | NA | Y | - | Y | café au lait patch |
| P12 | 9 | F | 12 | Y | Y | Y | - | N | - |
| P13 | 10 | M | 22 | Y | Y | Y | Y | N | DDH, café au lait patch |
| P14 | 11 | F | 18 | Y | Y | Y | - | Y | gastrostomy, hypercalcaemia in infancy, café au lait patches, DDH, kyphoscoliosis |
| P15 | 12 | M | 31 | Y | NA | Y | Y | Y | café au lait patches, seizures, osteopenia, osteoporosis, nodular sclerosis, Hodgkin's lymphoma |

Abbreviations: ID, individual number; Fam, family number; I, intrauterine growth restriction; M_{+SI}, skeletal involvement: metaphyseal dysplasia or other skeletal abnormalities reported in CDKN1C IMAGE-affected individuals (NA, not assessed); A, adrenal insufficiency; Ge, genitourinary abnormalities in males (- female, genitourinary anomalies not applicable); -I, immunodeficiency, either increased susceptibility to infections or documented lymphopenia/hypogammaglobinemia; DDH, developmental dysplasia of the hip; Y, yes; N, no. See Tables S1–S4 for extended clinical data and morphometrics.

DNA in the variant transcript results in a frameshift, which would lead to premature termination (p.Asn563Valfs*16). While this transcript might be targeted for nonsense-mediated decay, any translated protein would also be non-functional given that this frameshift occurs at the start of the polymerase catalytic domain. Combined with a LoF mutation on the second allele, substantial reduction in POLE1 was therefore anticipated. Subsequent immunoblotting of total protein extracts from primary fibroblasts from affected subjects confirmed that POLE1 levels were indeed markedly depleted (Figure 3; 5% ± 3% for P1 and 11% ± 4% P3, relative to the mean of both control subjects and normalized to vinculin loading control; mean ± SD for n = 2 independent experiments), with chromatin fractionation experiments demonstrating reduction of POLE1 in both soluble and chromatin-bound fractions (Figure S4). Taken together with the consistent clinical phenotype across case subjects, we concluded that the identified *POLE* variants were pathogenic, resulting in a phenotype spectrum substantially overlapping IMAGE syndrome.

In keeping with an essential requirement for *POLE* in eukaryotes,² the “leaky” c.1686+32C>G splice mutation

permitted residual expression of functional POLE1 in all case subjects. This mutation in *trans* with truncating mutations would then be expected to lead to marked but partial loss of function. As *POLE* encodes POLE1, the catalytic subunit of the major leading-strand DNA polymerase Pol ε, reduced chromatin levels of POLE1 would therefore be expected to impact on the availability of Pol ε DNA polymerase activity during its canonical function in DNA replication. Consistent with this, time-course FACS analysis demonstrated delayed cell-cycle progression of BrdU-labeled primary fibroblasts from P1 and P3, indicative of impaired S-phase progression (Figure 3). While no viable model of POLE1 deficiency exists, a *Pole4*^{-/-} mouse has been generated, which is similarly deficient for the Pol ε holoenzyme.¹⁷ This mouse also has significant prenatal onset growth failure, reduced brain size, and markedly reduced lymphocyte levels. Analysis of embryonic fibroblasts derived from this mouse alongside *POLE* primary human fibroblasts (derived from P1 and P3 in this study) established that in both cases Pol ε deficiency leads to reduced levels of chromatin-loaded Pol ε complexes, resulting in replication stress arising from reduced numbers of active replication origins.¹⁷

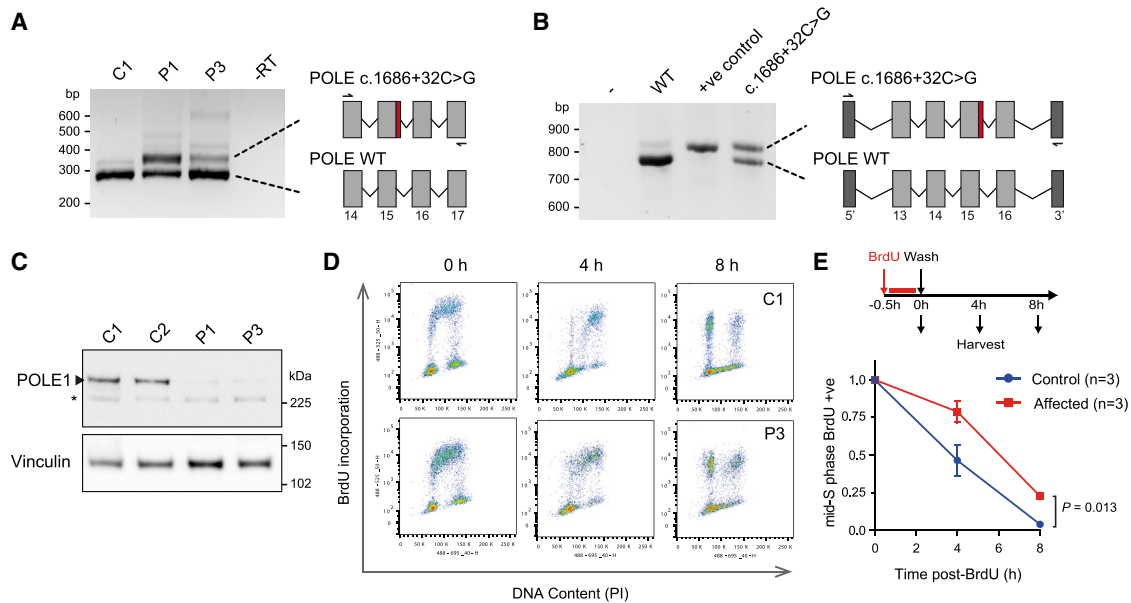


Figure 3. Common Intronic Variant Identified Causes Aberrant Splicing and *POLE*-Deficient Cells Show Deficiency of Polymerase Epsilon and Slowed S-phase Progression

(A) The c.1686+32C>G mutation causes aberrant splicing of intron 15 in subject cells. RT-PCR of *POLE* transcripts from primary fibroblasts. Primers indicated by arrows in schematic. P1, P3, *POLE*-deficient subjects; C1, C2, control subjects.
 (B) Minigene assay demonstrating that aberrant splicing is a direct consequence of the c.1686+32C>G mutation. +ve control, point mutation in splice donor site, c.1686+1G>A. 5' & 3' indicate artificial vector-associated exons.
 (C) *POLE1* levels are markedly reduced in subject fibroblasts. Immunoblot of total cell extracts. *POLE1* antibody raised against AA1-176. Vinculin, loading control. * non-specific band.
 (D and E) Fibroblast cells from affected individuals exhibit delayed S phase progression. Schematic, experimental set-up.
 (D) Representative FACS plots.
 (E) Quantification of n = 3 affected and n = 3 control cell lines from representative experiment (of n = 3 expts with n ≥ 2 biological replicates per group). Mid-S-phase mean (± SEM) BrdU-labeled cells, normalized to t = 0 time point are plotted for each group. p value, two-way ANOVA.

IMAge syndrome has previously been found to be caused by dominant gain-of-function mutations in the imprinted gene, *CDKN1C*.^{18,19} Here, we establish mutations of *POLE* as an autosomal-recessive cause of the IMAge phenotype. These mutations contrast with heterozygous germline and somatic cancer-predisposing mutations that affect the exonuclease domain of *POLE1*^{3–6} (Figure 1). IMAge and cancer mutations are likely to have differing functional outcomes, respectively leading to deficient DNA replication or to impaired proof-reading.²⁰ Hence, a similar cancer predisposition in *POLE1*-deficient individuals or *POLE* heterozygous carriers cannot be assumed. However, P5 developed a T cell lymphoma at age 11 and P15 developed Hodgkin's lymphoma at age 28. Given also the increased lymphoma rates in *Pole4*^{-/-} mice,¹⁷ *POLE1* deficiency may therefore confer an increased risk of lymphoma.

All *CDKN1C* IMAge mutations cluster within its proliferating cell nuclear antigen (PCNA) binding domain,^{18,19} targeting the PCNA binding PIP-box motif.²¹ As PCNA loads with Pol ε at replication initiation (Figures 4 and S5), the phenotypic overlap with *POLE*-associated IMAge syndrome suggests a mechanistic link. Supporting this notion, biochemical studies of a *Xenopus* homolog suggests that CDKN ubiquitination and subsequent degradation

is mediated by PCNA/polymerase loading^{23,24} (Figure S5). Furthermore, single homozygous mutations in *MCM4*^{11,25} (MIM: 609981) and *POLE2*²⁶ have been associated with IUGR and short stature, alongside immunodeficiency, respectively with and without adrenal failure. Likewise, several families with *GINS1* biallelic mutations have been reported to be associated with pre/postnatal growth restriction, chronic neutropenia, and NK cell deficiency (MIM: 610608).¹⁰ Hence, the identification of a cohort of individuals with *POLE* mutations that encompasses all these features consolidates this as a group of replisome-associated disorders (Figure 4, Table S5). Replication stress and p53-mediated cell death¹⁷ likely explain the immunodeficiency as well as global growth failure in *POLE1*-deficient individuals. However, why impaired replisome function should have a particularly strong impact on specific lymphoid lineages (T/B cells in *POLE1/2*-deficient subjects and NK cells in *MCM4/GINS1*-deficient individuals) or on adrenal cortical cells is unclear. Notably, another distinct form of primordial dwarfism, Meier-Gorlin syndrome (defined by the triad of short stature, patella hypoplasia, and microtia [MIM: 224690]) is also caused by biallelic (or *de novo*) mutations in genes involved in replication licensing and initiation^{7–9,27,28} (Figure 4). Further studies to understand the specific role(s) of the encoded

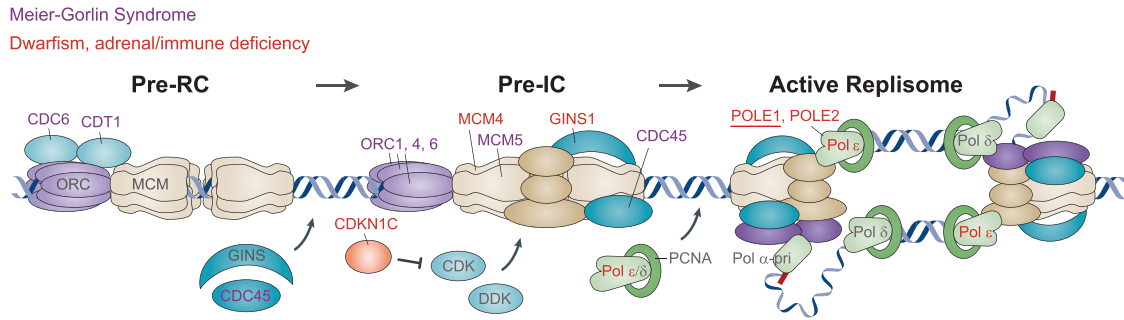


Figure 4. POLE1 Deficiency Links CDKN1C-IMAGE Syndrome¹⁸ with Other Replisome-Associated Disorders

Schematic of replication initiation (adapted by permission from Gaillard et al.²² copyright 2015 Macmillan Publishers), highlighting the sequential action of replisome-associated proteins, mutation of which causes MGS (blue text) and those that are associated with dwarfism with adrenal insufficiency and/or immune deficiency, including IMAGE syndrome (red text). During replication licensing, MCM helicases (MCM2-7) are loaded at replication origins by the ORC complex (ORC1-6) with CDC6 and CDT1 to form the pre-replicative complex (pre-RC). Subsequently, loading of additional replisome protein occurs, regulated by DDK and CDK kinases, to form the pre-initiation complex (pre-IC), that contains the CMG (CDC45, MCMs, GINS) complex. CDKN1C inhibits CDK activity. In the active replisome, Primase-Pol α initiates DNA synthesis with strands extended by the PCNA-associated DNA polymerases δ and ϵ . POLE1 and POLE2 are part of the Pol ϵ holoenzyme.

replication proteins during development, along with the cellular and biochemical basis for the relationship between CDKN1C and Pol ϵ , will therefore be of interest.

Supplemental Data

Supplemental Data include Supplemental Note, seven figures, five tables, and Supplemental Material and Methods and can be found with this article online at <https://doi.org/10.1016/j.ajhg.2018.10.024>.

Consortia

Members of the Scottish Genome Partnership include Timothy J. Aitman, Andrew V. Biankin, Susanna L. Cooke, Wendy Inglis Humphrey, Sancha Martin, Lynne Mennie, Alison Meynert, Zosia Miedzobrodzka, Fiona Murphy, Craig Nourse, Javier Santoyo-Lopez, Colin A. Semple, and Nicola Williams.

Acknowledgments

We thank the families and clinicians for their involvement and participation; the Potentials Foundation and Walking with Giants Foundation; D. Fitzpatrick, N. Hastie, and W. Bickmore for discussions; E. Freyer for assistance with FACS analysis; IGMM core sequencing service; and Edinburgh Genomics (Clinical Division) for WGS sequencing. We thank Penny Jeggo for sharing cell lines. This work was supported by funding to the Jackson lab from European Research Council ERC Starter Grant HumGenSize, 281847; ERC Advanced Investigator Grant GrowCell, 788093; by a UK Medical Research Council Human Genetics Unit core grant (MRC, U127580972), and the Scottish Genomes Partnership. The Rios lab is supported by Texas Scottish Rite Hospital for Children and the Children's Medical Center Foundation. Research reported in this publication was supported by the National Center for Advancing Translational Sciences of the National Institutes of Health under award number UL1TR001105. The content is solely the responsibility of the authors and does not necessarily represent the official views of the NIH. Boulton lab work is supported by the Francis Crick Institute, which receives its core fund-

ing from Cancer Research UK (FC0010048), the UK Medical Research Council (FC0010048), and the Wellcome Trust (FC0010048); a European Research Council (ERC) Advanced Investigator Grant (TelMetab); and Wellcome Trust Senior Investigator and Collaborative Grants. R.K.S. is funded by the Wellcome Trust (210752/Z/18/Z). The Scottish Genomes Partnership is funded by the Chief Scientist Office of the Scottish Government Health Directorates (SGP/1) and The Medical Research Council Whole Genome Sequencing for Health and Wealth Initiative.

Declaration of Interests

The Department of Molecular and Human Genetics at Baylor College of Medicine receives revenue from the genetic testing services offered by Baylor Genetics.

Received: August 6, 2018

Accepted: October 26, 2018

Published: November 29, 2018

Web Resources

dbSNP, <https://www.ncbi.nlm.nih.gov/projects/SNP/>
 GenBank, <https://www.ncbi.nlm.nih.gov/genbank/>
 GeneReviews, Bennett, J., Schrier Vergano, S.A., and Dearnorff, M.A. (1993). IMAGE syndrome, <https://www.ncbi.nlm.nih.gov/books/NBK190103/>
 gnomAD Browser, <http://gnomad.broadinstitute.org/>
 OMIM, <http://www.omim.org/>

References

- Burgers, P.M.J., and Kunkel, T.A. (2017). Eukaryotic DNA replication fork. *Annu. Rev. Biochem.* 86, 417–438.
- Hogg, M., and Johansson, E. (2012). DNA polymerase ϵ . *Subcell. Biochem.* 62, 237–257.
- Palles, C., Cazier, J.B., Howarth, K.M., Domingo, E., Jones, A.M., Broderick, P., Kemp, Z., Spain, S.L., Guarino, E., Salguero, I., et al.; CORGI Consortium; and WGS500 Consortium (2013). Germline mutations affecting the proofreading

- domains of POLE and POLD1 predispose to colorectal adenomas and carcinomas. *Nat. Genet.* **45**, 136–144.
4. Church, D.N., Briggs, S.E., Palles, C., Domingo, E., Kearsey, S.J., Grimes, J.M., Gorman, M., Martin, L., Howarth, K.M., Hodgson, S.V., et al.; NSECG Collaborators (2013). DNA polymerase ϵ and δ exonuclease domain mutations in endometrial cancer. *Hum. Mol. Genet.* **22**, 2820–2828.
 5. Bellido, F., Pineda, M., Aiza, G., Valdés-Mas, R., Navarro, M., Puente, D.A., Pons, T., González, S., Iglesias, S., Darder, E., et al. (2016). POLE and POLD1 mutations in 529 kindred with familial colorectal cancer and/or polyposis: review of reported cases and recommendations for genetic testing and surveillance. *Genet. Med.* **18**, 325–332.
 6. Cancer Genome Atlas, N.; and Cancer Genome Atlas Network (2012). Comprehensive molecular characterization of human colon and rectal cancer. *Nature* **487**, 330–337.
 7. Bicknell, L.S., Bongers, E.M., Leitch, A., Brown, S., Schoots, J., Harley, M.E., Aftimos, S., Al-Aama, J.Y., Bober, M., Brown, P.A., et al. (2011). Mutations in the pre-replication complex cause Meier-Gorlin syndrome. *Nat. Genet.* **43**, 356–359.
 8. Bicknell, L.S., Walker, S., Klingseisen, A., Stiff, T., Leitch, A., Kerzendorfer, C., Martin, C.A., Yeyati, P., Al Sanna, N., Bober, M., et al. (2011). Mutations in ORC1, encoding the largest subunit of the origin recognition complex, cause microcephalic primordial dwarfism resembling Meier-Gorlin syndrome. *Nat. Genet.* **43**, 350–355.
 9. Fenwick, A.L., Kliszczak, M., Cooper, F., Murray, J., Sanchez-Pulido, L., Twigg, S.R.F., Goriely, A., McGowan, S.J., Miller, K.A., Taylor, I.B., et al.; WGS500 Consortium (2016). Mutations in CDC45, Encoding an Essential Component of the Pre-initiation Complex, Cause Meier-Gorlin Syndrome and Craniosynostosis. *Am. J. Hum. Genet.* **99**, 125–138.
 10. Cottineau, J., Kottemann, M.C., Lach, F.P., Kang, Y.H., Vély, F., Deenick, E.K., Lazarov, T., Gineau, L., Wang, Y., Farina, A., et al. (2017). Inherited GINS1 deficiency underlies growth retardation along with neutropenia and NK cell deficiency. *J. Clin. Invest.* **127**, 1991–2006.
 11. Gineau, L., Cognet, C., Kara, N., Lach, F.P., Dunne, J., Veturi, U., Picard, C., Trouillet, C., Eidenschenk, C., Aoufouchi, S., et al. (2012). Partial MCM4 deficiency in patients with growth retardation, adrenal insufficiency, and natural killer cell deficiency. *J. Clin. Invest.* **122**, 821–832.
 12. Lek, M., Karczewski, K.J., Minikel, E.V., Samocha, K.E., Banks, E., Fennell, T., O'Donnell-Luria, A.H., Ware, J.S., Hill, A.J., Cummings, B.B., et al.; Exome Aggregation Consortium (2016). Analysis of protein-coding genetic variation in 60,706 humans. *Nature* **536**, 285–291.
 13. Tan, T.Y., Jameson, J.L., Campbell, P.E., Ekert, P.G., Zacharin, M., and Savarirayan, R. (2006). Two sisters with IMAGe syndrome: cytomegalic adrenal histopathology, support for autosomal recessive inheritance and literature review. *Am. J. Med. Genet. A.* **140**, 1778–1784.
 14. Pedreira, C.C., Savarirayan, R., and Zacharin, M.R. (2004). IMAGe syndrome: a complex disorder affecting growth, adrenal and gonadal function, and skeletal development. *J. Pediatr.* **144**, 274–277.
 15. Pachlopnik Schmid, J., Lemoine, R., Nehme, N., Cormier-Daire, V., Revy, P., Debeurme, F., Debré, M., Nitschke, P., Bole-Feysot, C., Legeai-Mallet, L., et al. (2012). Polymerase ϵ 1 mutation in a human syndrome with facial dysmorphism, immunodeficiency, livedo, and short stature (“FILS syndrome”). *J. Exp. Med.* **209**, 2323–2330.
 16. Thiffault, I., Saunders, C., Jenkins, J., Rajé, N., Canty, K., Sharma, M., Grote, L., Welsh, H.I., Farrow, E., Twist, G., et al. (2015). A patient with polymerase E1 deficiency (POLE1): clinical features and overlap with DNA breakage/instability syndromes. *BMC Med. Genet.* **16**, 31.
 17. Bellelli, R., Borel, V., Logan, C., Svendsen, J., Cox, D.E., Nye, E., Metcalfe, K., O'Connell, S.M., Stamp, G., Flynn, H.R., et al. (2018). Pole Instability Drives Replication Stress, Abnormal Development, and Tumorigenesis. *Mol. Cell* **70**, 707–721.e7.
 18. Arboleda, V.A., Lee, H., Parnaik, R., Fleming, A., Banerjee, A., Ferraz-de-Souza, B., Délot, E.C., Rodríguez-Fernandez, I.A., Braslavsky, D., Bergadá, I., et al. (2012). Mutations in the PCNA-binding domain of CDKN1C cause IMAGe syndrome. *Nat. Genet.* **44**, 788–792.
 19. Hamajima, N., Johmura, Y., Suzuki, S., Nakanishi, M., and Saitoh, S. (2013). Increased protein stability of CDKN1C causes a gain-of-function phenotype in patients with IMAGe syndrome. *PLoS ONE* **8**, e75137.
 20. Shcherbakova, P.V., Pavlov, Y.I., Chilkova, O., Rogozin, I.B., Johansson, E., and Kunkel, T.A. (2003). Unique error signature of the four-subunit yeast DNA polymerase epsilon. *J. Biol. Chem.* **278**, 43770–43780.
 21. Borges, K.S., Arboleda, V.A., and Vilain, E. (2015). Mutations in the PCNA-binding site of CDKN1C inhibit cell proliferation by impairing the entry into S phase. *Cell Div.* **10**, 2.
 22. Gaillard, H., García-Muse, T., and Aguilera, A. (2015). Replication stress and cancer. *Nat. Rev. Cancer* **15**, 276–289.
 23. Furstenthal, L., Swanson, C., Kaiser, B.K., Eldridge, A.G., and Jackson, P.K. (2001). Triggering ubiquitination of a CDK inhibitor at origins of DNA replication. *Nat. Cell Biol.* **3**, 715–722.
 24. Chuang, L.C., and Yew, P.R. (2005). Proliferating cell nuclear antigen recruits cyclin-dependent kinase inhibitor Xic1 to DNA and couples its proteolysis to DNA polymerase switching. *J. Biol. Chem.* **280**, 35299–35309.
 25. Hughes, C.R., Guasti, L., Meimaridou, E., Chuang, C.H., Schimenti, J.C., King, P.J., Costigan, C., Clark, A.J., and Metherell, L.A. (2012). MCM4 mutation causes adrenal failure, short stature, and natural killer cell deficiency in humans. *J. Clin. Invest.* **122**, 814–820.
 26. Frugoni, F., Dobbs, K., Felgentreff, K., Aldhekri, H., Al Saud, B.K., Arnaout, R., Ali, A.A., Abhyankar, A., Alroqi, F., Giliani, S., et al. (2016). A novel mutation in the POLE2 gene causing combined immunodeficiency. *J. Allergy Clin. Immunol.* **137**, 635–638.e1.
 27. Guernsey, D.L., Matsuoka, M., Jiang, H., Evans, S., Macgillivray, C., Nightingale, M., Perry, S., Ferguson, M., LeBlanc, M., Paquette, J., et al. (2011). Mutations in origin recognition complex gene ORC4 cause Meier-Gorlin syndrome. *Nat. Genet.* **43**, 360–364.
 28. Burrage, L.C., Charng, W.L., Eldomery, M.K., Willer, J.R., Davis, E.E., Lugtenberg, D., Zhu, W., Leduc, M.S., Akdemir, Z.C., Azamian, M., et al. (2015). De Novo GMNN Mutations Cause Autosomal-Dominant Primordial Dwarfism Associated with Meier-Gorlin Syndrome. *Am. J. Hum. Genet.* **97**, 904–913.